

# MimiQ: Low-Bit Data-Free Quantization of Vision Transformers with Encouraging Inter-Head Attention Similarity

Kanghyun Choi<sup>1</sup>, Hye Yoon Lee<sup>1</sup>, Dain Kwon<sup>1</sup>, SunJong Park<sup>1</sup>, Kyuyeun Kim<sup>2</sup>, Noseong Park<sup>3</sup>, and Jinho Lee<sup>1</sup>

<sup>1</sup> Seoul National University

{kanghyun.choi, hylee817, dain.kwon, ryan0507, leejinho}@snu.ac.kr

<sup>2</sup> Google

kyuyeunk@google.com

<sup>3</sup> KAIST

noseong@kaist.ac.kr

**Abstract.** Data-free quantization (DFQ) is a technique that creates a lightweight network from its full-precision counterpart without the original training data, often through a synthetic dataset. Although several DFQ methods have been proposed for vision transformer (ViT) architectures, they fail to achieve efficacy in low-bit settings. Examining the existing methods, we identify that their synthetic data produce misaligned attention maps, while those of the real samples are highly aligned. From the observation of aligned attention, we find that aligning attention maps of synthetic data helps to improve the overall performance of quantized ViTs. Motivated by this finding, we devise MimiQ, a novel DFQ method designed for ViTs that focuses on inter-head attention similarity. First, we generate synthetic data by aligning head-wise attention responses in relation to spatial query patches. Then, we apply head-wise structural attention distillation to align the attention maps of the quantized network to those of the full-precision teacher. The experimental results show that the proposed method significantly outperforms baselines, setting a new state-of-the-art performance for data-free ViT quantization.

**Keywords:** Neural network compression · Data-free quantization · Vision transformer

## 1 Introduction

Over the past few years, the Vision Transformer (ViT) [14] has gained increasing interest among researchers, due to its remarkable performance on many computer vision tasks. However, ViT has high computational costs compared to conventional CNN networks, making it difficult to adopt in many resource-constrained devices (e.g., embedded systems). This has led to various works to focus on reducing the computational complexity of ViT architectures [21, 23, 30, 33, 48]. One popular approach is network quantization [2, 20, 28, 36], which converts full-precision floating-point parameters and features to low-bit integers. However,

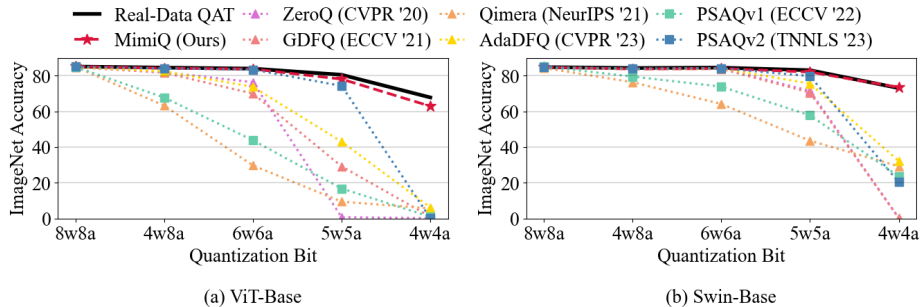


**Fig. 1:** Accuracy comparison of data-free quantization methods when applied to ViT architectures. We use quantization bitwidths commonly used in literature [4, 39, 46]. Not only do existing CNN-specific methods ( $\blacktriangle$ ) [4, 8, 39, 46] suffer from huge accuracy degradation in low-bit quantization, but ViT-aware DFQ methods ( $\blacksquare$ ) [24, 26] also show destructive behavior when used in low-bit settings. Best viewed in color.

naively converting the parameters to lower-bit induces a large accuracy drop, which is why quantization usually requires additional calibration [30, 33, 42] or fine-tuning [12, 16, 19] using the original training dataset. Unfortunately, in real-life cases, even if the network itself is accessible, the original training dataset is not always available for fine-tuning due to privacy concerns, security issues, copyright protections, or even dataset sizes [17, 31].

Data-free (or zero-shot) quantization (DFQ) [4, 8, 24, 26, 35, 39, 46, 50, 51] are methods that address such dataset inaccessibility by proposing to quantize the network without using the original training data. To replace the original training dataset, recent DFQ methods generate synthetic data from the pretrained networks and use it for calibration [8, 9, 46, 50, 51]. Some approaches directly optimize synthetic samples with gradient descent [4, 24, 26, 50, 51], while other approaches train an auxiliary generator model for sample generation [8, 39, 46].

However, current DFQ methods suffer from destructive accuracy drops in low-bit when applied to ViT architectures. We conducted an extensive comparison with two DFQ methods for ViTs [24, 26], which are only available baselines designed for ViTs, and four CNN-based DFQ methods [4, 8, 39, 46]. The experimental results are shown in Fig. 1. The DFQ methods for ViTs [24, 26] suffer from huge degradation in low-bit settings. Although there are some DFQ methods that are reported to achieve considerable accuracy in low-bit CNN settings [8, 39, 46], they experience similar accuracy drops when applied to ViTs.

To this end, we devise a novel DFQ method for ViT named MimiQ, which considers inter-head attention similarity in both dataset generation and quantization phases. By inspecting the attention maps resulting from real and synthetic data, we observe that aligning attention maps of synthetic samples contributes to increase in quantization accuracy. Inspired by this, we design a DFQ method that focuses on inter-head attention similarity. In dataset generation, we align inter-head attention maps by generating synthetic samples that minimize the distance between attention maps for each spatial query patch. For fine-tuning, we

employ head-wise attention distillation to minimize output distances, ensuring the quantized network accurately mimics its full-precision counterpart.

We evaluate our method on extensive experiments covering various tasks, ViT architectures, and quantization settings. The experimental results show that our method outperforms baselines by a significant margin in low-bit settings. Furthermore, MimiQ generally shows the best accuracy compared to the baselines, reducing the gap between data-free and real-data quantization. As a result, MimiQ sets a new state-of-the-art result for the data-free ViT quantization task.

Our primary contributions are summarized as follows:

- We discover that alignment on attention maps across attention heads contributes to the data-free quantization accuracy, especially in low-bit settings.
- We propose a synthetic data generation method that aims to produce samples towards inter-head attention similarity by reducing distance between attention head outputs in relation to spatial query patches.
- We propose a head-wise attention distillation method for quantized network fine-tuning by aligning structure of attention head outputs of quantized networks with those of full-precision teachers.
- We conduct experiments on multiple tasks with various ViT architecture and quantization settings. The extensive experimental results show that MimiQ achieves new state-of-the-art performance for data-free ViT quantization.

## 2 Preliminaries

### 2.1 Vision Transformers and Multi-Head Attention

Vision Transformers (ViT) [14, 32, 43] are adaptations of Transformer architectures from NLP tasks [3, 13] to vision. Each Transformer block comprises two consecutive layers: a multi-head self-attention (MSA) layer and a feed-forward (FF) layer. The MSA layer performs attention using multiple heads for the length  $N_d$  input sequence with  $d$ -dimension,  $X_{\in N_d \times d}$ , to obtain diverse representations from each head as follows:

$$MSA(X) = [H_1(X), \dots, H_N(X)]W^O, \quad (1)$$

where  $N$  is the number of attention heads. The outputs of each head are concatenated ( $[ \cdot ]$ ) and merged by multiplication with projection matrix  $W^O$ . Each attention head has separated weights ( $W_h^Q, W_h^K, W_h^V$ ) for computing query, key, and value vectors. For input sequence  $X$ , the output of  $h$ -th head is as follows:

$$(Q_h, K_h, V_h) = (XW_h^Q, XW_h^K, XW_h^V) \quad (2)$$

$$H_h(X) = softmax\left(\frac{Q_h K_h^T}{\sqrt{d}}\right)V_h. \quad (3)$$

### 2.2 Data-Free Quantization

**Quantization** reduces network complexity by converting floating-point to integer operations, decreasing storage needs, and improving computational efficiency [5, 10, 15, 20, 34–36, 40, 53]. We employ uniform quantization which uses a

simple scale ( $s$ ) and zero-point ( $z$ ) mapping to transform floating-point values  $\theta$  into integers  $\theta^{int}$ :

$$\theta^{int} = \text{clamp}(\lfloor \theta \cdot s - z \rfloor, q_{min}, q_{max}), \quad (4)$$

where  $(q_{min}, q_{max})$  indicates minimum and maximum values of the integer representation range, i.e.,  $(-2^{k-1}, 2^{k-1} - 1)$ . For more details, please refer to Sec. 10 in Appendix. However, please note that our work is independent of the quantization method. One drawback of quantization is that it can lead to accuracy loss due to the reduction in data precision. To counter this, quantization-aware training (QAT) [5, 15, 20, 40, 53] uses fine-tuning to regain lost accuracy. However, the training dataset is not always available in real-life scenarios [17, 31], making QAT inapplicable.

**Data-free quantization** aims to quantize a pretrained full-precision network into lower-bit integers without access to any of the real training data. Frequently, this is achieved by using synthetic samples as surrogates to the real training dataset. The major challenge is that one cannot use the training data or external generators for the synthesis, as it would fall into a case of data leakage. Instead, information drawn from the full precision network is used by setting the following terms as optimization objectives [4, 26, 46, 47, 51].

$$\mathcal{L}_{CL} = - \sum_c^C \hat{y}_c \log(f(\hat{x})_c), \quad (5)$$

$$\begin{aligned} \mathcal{L}_{TV} = & \|I_{h,w} - I_{h+1,w}\|_2^2 + \|I_{h,w} - I_{h,w+1}\|_2^2 \\ & + \|I_{h,w} - I_{h+1,w+1}\|_2^2 + \|I_{h,w} - I_{h+1,w-1}\|_2^2, \end{aligned} \quad (6)$$

$$\mathcal{L}_{BNS} = \|\hat{\mu}_l - \mu_l\|_2^2 + \|\hat{\sigma}_l - \sigma_l\|_2^2, \quad (7)$$

where  $f$  is the given full-precision network,  $I$  is the synthetic image being generated,  $y_c$  is a class label we want to generate among  $C$  classes,  $(h, w)$  are pixel coordinates of the image, and  $(\mu, \sigma)$  are BN statistics.  $\mathcal{L}_{CL}$  embeds prior knowledge of the pretrained classifier, and  $\mathcal{L}_{TV}$  prevents steep changes between nearby pixels.  $\mathcal{L}_{BNS}$  reduces the distance between feature statistics of synthetic samples and BN layers. They are used to optimize images [4, 47, 51] or to train a generator [8, 46], but  $\mathcal{L}_{BNS}$  is not applicable to ViTs due to its lack of BN layers.

## 3 Related Work

### 3.1 Vision Transformer Quantization

After the success of ViTs, many efforts have been followed to reduce its expensive computational and memory cost through quantization. One of the pioneering efforts is PTQ-ViT [33], which performed quantization to preserve the functionality of the attention mechanism. Then followed FQ-ViT [30], which proposed to fully quantize ViT including LayerNorm and Softmax. PTQ4ViT [49] applied

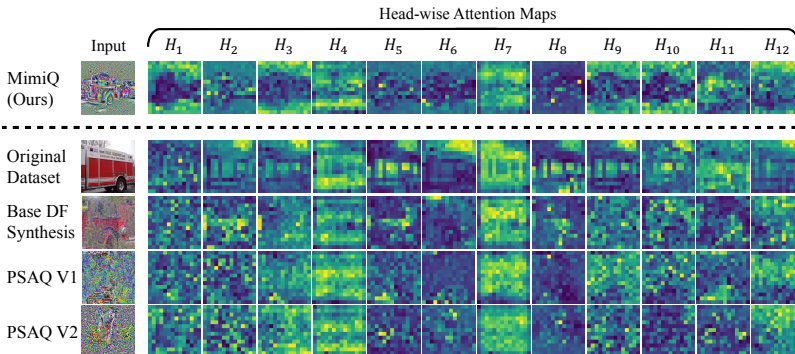


**Fig. 2:** Attention map visualization of synthetic samples and the original dataset. Compared to the original dataset, synthetic data from existing DFQ methods present misaligned attention maps. The first row denotes attention maps extracted from samples generated by MimiQ, showing aligned attention maps among attention heads.

twin uniform quantization strategy and Hessian-based metric for determining quantization scaling factor. I-ViT [25] performed integer-only quantization with complete absence of any floating-point arithmetic. Q-ViT [23] and RepQ-ViT [27] proposed remedies to overcome accuracy degradation in low-bit ViTs. However, they require the original training data for calibration, and do not consider real-life scenarios where training data is often unavailable.

### 3.2 Data-Free Quantization of Vision Transformers

After DFQ [35]’s first proposal for data-free quantization problem, many efforts specialized for CNNs have followed, including ZeroQ [4], DSG [50], and intraQ [51]. Notably, GDFQ [46] proposed to jointly train generators to synthesize samples, which laid foundation for variants using better generator [54], boundary samples [8], smooth loss surface [9], and sample adaptability [39]. This stream of methods owe a large portion of its success to the technique that utilizes the statistics stored in the BN layers (Eq. (7)) [4].

Unfortunately, BN layer is absent in ViT architectures, making existing CNN-targeted techniques suffer from inaccurate sample distribution when adopted to ViTs. To the best of our knowledge, DFQ for ViT is still in an early stage of development, with only two prior works in existent. PSAQ-ViT [26] was the first to present DFQ for ViTs, proposing inter-patch discrepancy of foreground and background patches to generate realistic samples. The following work PSAQ-ViT V2 [24] improved this using an adaptive method by applying the concept of adversarial training. Although they have shown successful results in 8-bit quantization, their method suffers from drastic accuracy drop in low-bit quantization.

## 4 Motivational Study

As previously discussed with Fig. 1, all the baseline DFQ methods experience huge accuracy drops in low-bit settings compared to the real-data QAT using

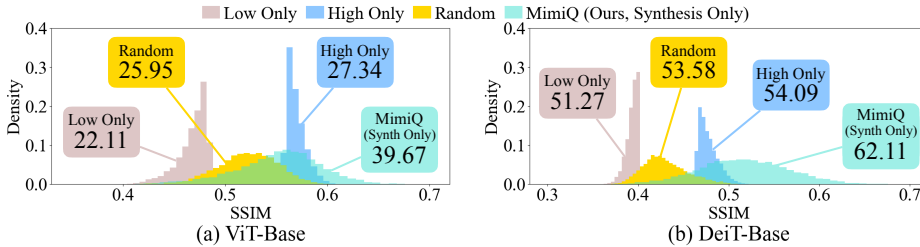


**Fig. 3:** Histogram comparing four synthetic datasets: high attention similarity, low attention similarity, randomly sampled from whole distribution, samples generated by MimiQ. Colored boxes denote test accuracy on ImageNet when trained using only the samples in the corresponding dataset. MimiQ shows the best performance whilst having the highest attention similarity.

the original training dataset. To investigate the source of such discrepancy, we inspect the internal attention behavior of ViTs. Specifically, we study the ViT’s head-wise attention maps of the MSA layers denoted as  $H_i$  in Eq. (1).

The visualization in Fig. 2 show that real samples lead to similarly structured attention maps, unlike data-free synthetic samples. We first set the base data-free synthesis method, which generates synthetic samples with  $\mathcal{L}_{CL}$  (Eq. (5)) and  $\mathcal{L}_{TV}$  (Eq. (6)) through gradient-based optimization. We also analyze two DFQ baseline methods for ViT [24, 26]. On the one hand, the attention maps drawn from real images clearly display the object’s structure in most heads. While minor variations are caused by differences of heads highlighting either the object itself (e.g.,  $H_{11}$ ) or the background (e.g.,  $H_9$ ), they exhibit overall coherence and high similarity to one another. On the other hand, synthetic samples from data-free methods (Base synthesis, PSAQ-ViT, PSAQ-ViT V2) do not seem to produce visually similar attention maps among attention heads. The visualizations in Fig. 2 are conducted with ViT-Base architecture with 12 attention heads. Refer to Sec. 15 for more visualization on other ViT architectures.

From the observation in Fig. 2, we hypothesize that aligning inter-head attention from synthetic samples contributes to better accuracy of data-free quantized ViT networks. To validate this, we performed motivational experiments to identify the correlation between attention map alignment and quantization accuracy. First, we generate a synthetic dataset using the base synthesis mentioned above. We then measure the inter-head attention similarity of each image with [45] and construct subsets of the synthetic dataset having 1) high attention similarity and 2) low attention similarity. For comparison, we construct a control group with 3) uniform random selection. Lastly, we train a W4/A4 quantized ViT network with each sampled group and examine the quantization accuracy.

The motivational experiments are shown in Fig. 3. The results show that quantized networks trained with low attention similarity samples consistently underperform compared to networks trained with samples of high attention similarity. These results empirically validate our hypothesis that the inter-head attention similarity of synthetic samples correlates with the quantization accuracy. Based on the observation, MimiQ encourages inter-head attention simi-

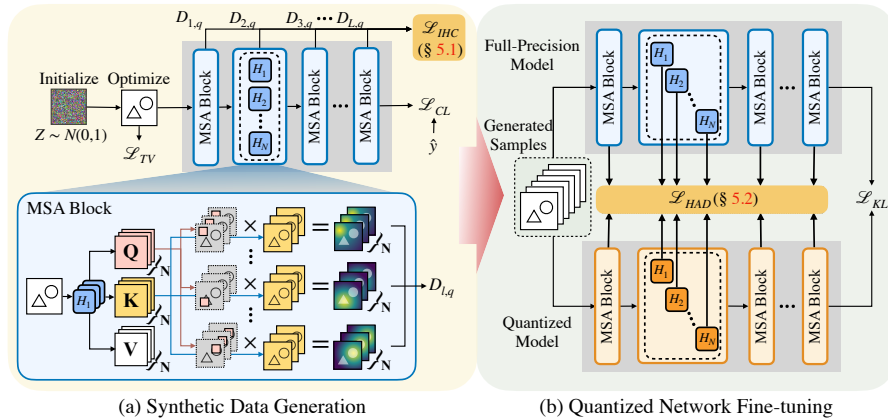


**Fig. 4:** An overview of the proposed method. (a) demonstrates the proposed synthetic data generation method (Sec. 5.1). The synthetic sample is initialized with Gaussian random noise, then optimized with class loss ( $\mathcal{L}_{CL}$ ), total variance loss ( $\mathcal{L}_{TV}$ ), and the proposed inter-head coherency loss  $\mathcal{L}_{IHC}$ . (b) depicts quantized network fine-tuning with generated synthetic samples (Sec. 5.2). The quantized network is trained to minimize output discrepancy ( $\mathcal{L}_{KL}$ ) and inter-head discrepancy ( $\mathcal{L}_{HAD}$ ) to reduce the gap between the full-precision network and the quantized counterpart.

larity throughout the whole DFQ process, including both data generation and fine-tuning phases. As shown with turquoise bars in Fig. 3, samples generated with method of MimiQ yield higher attention similarity while having superior quantization accuracy. In the next section, we will describe the details with an additional distillation method to further improve the performance.

## 5 Proposed Method

Inspired by the observation from Sec. 4, we propose a simple but effective method named MimiQ, a data-free quantization method for the ViTs that extracts knowledge from MSA layers of a pretrained full-precision network. The overall process is depicted in Fig. 4. We devise a synthetic data generation scheme designed for ViT architectures that directly minimizes inter-head attention discrepancy of MSA layers (Sec. 5.1). Furthermore, we propose a fine-tuning scheme for a quantized network in Sec. 5.2, which employs fine-grained head-level attention transfer between the full-precision teacher and the quantized student.

### 5.1 Sample Synthesis with Inter-Head Attention Similarity

We propose synthetic sample generation enhanced with inter-head attention similarity by aligning attention maps sharing the same spatial query patch index. The left side of Fig. 4 depicts attention head alignment. First, we collect attention maps from each head in relation to spatial query patch index  $q$ :

$$A_q = [Q_{1,q}K_1^\top \quad Q_{2,q}K_2^\top \quad \cdots \quad Q_{N,q}K_N^\top], \quad (8)$$

where  $A_q$  is the collected attention map and  $(Q, K)$  are query and key matrices from Eq. (2), respectively. Then, we measure the average distance  $D_q$  with attention distance metric  $f_{dist}$  between the attention heads as follows:

$$D_q = \frac{1}{N^2} \sum_i^N \sum_j^N f_{dist}(A_{q,i}, A_{q,j}). \quad (9)$$

Effective attention distance metrics need to consider the nature of attention maps: Attention maps can be inverted while retaining the structure of input images. For example, in the original sample in Fig. 2,  $H_{11}$  focuses on an object while  $H_9$  focuses on the background. Since the two attention maps share the same structure, the metric should also consider them as similar.

To this end, we use absolute structural similarity index measure (SSIM) [45] as  $f_{dist}$ . SSIM satisfies the requirement to capture both the positive and negative (inverted) correlations between the attention maps. A higher magnitude of SSIM indicates higher correlation in both positive and negative direction, thus representing the structural similarity between two attention maps. Using Eq. (9), we can optimize synthetic samples towards inter-head attention similarity with synthesized loss  $\mathcal{L}_G$ , comprises  $\mathcal{L}_{CL}$ ,  $\mathcal{L}_{TV}$ , and inter-head coherency loss  $\mathcal{L}_{IHC}$ :

$$\mathcal{L}_G = \mathcal{L}_{IHC} + \alpha \mathcal{L}_{CL} + \beta \mathcal{L}_{TV}, \quad (10)$$

$$\mathcal{L}_{IHC} = \frac{1}{LQ} \sum_l^L \sum_q^Q (1 - D_{l,q}), \quad (11)$$

where  $\alpha$  and  $\beta$  are hyperparameters for  $\mathcal{L}_{CL}$  and  $\mathcal{L}_{TV}$ , respectively,  $L$  is the number of MSA layers in ViT architecture, and  $D_{l,q}$  is  $D_q$  from layer  $l$ . The generated synthetic samples can be found in Fig. 6 and Sec. 10 in Appendix.

## 5.2 Structural Attention Head Distillation

On top of our inter-head aligned samples, we propose to use head-level structural distillation from a full-precision teacher to its quantized counterpart. In addition to the output matching loss (i.e.,  $\mathcal{L}_{KL}$ ) commonly adopted for fine-tuning the quantized network, we further reduce the distance  $g_{dist}$  between each attention output pair by optimizing the following objective:

$$\mathcal{L}_{HAD} = \frac{1}{LN} \sum_l^L \sum_i^N g_{dist}(H_{l,i}^T, H_{l,i}^S), \quad (12)$$

where  $\mathcal{L}_{HAD}$  is head-wise attention distillation loss.  $H_{l,i}^T$  and  $H_{l,i}^S$  are  $i$ -th attention head output from  $l$ -th layer of teacher and student, respectively.

We compare four candidate metrics for  $g_{dist}$ : Mean-squared error (MSE), L1 distance, KL-divergence, and structural dissimilarity (DSSIM), which is defined as the negative of absolute SSIM. Unlike  $f_{dist}$  where we have concrete required characteristic that it should be invariant of color inversion,  $g_{dist}$  is meant to



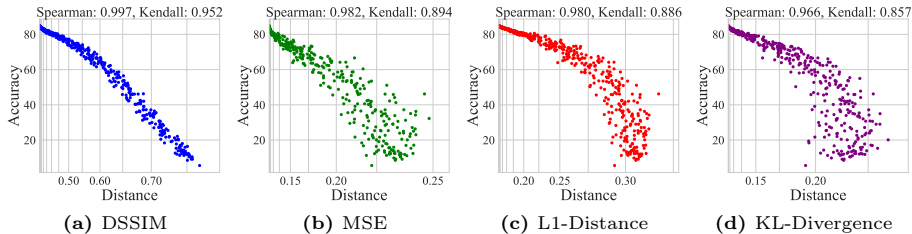


**Fig. 5:** This figure illustrates the comparison of four different attention coherency metrics: (a) DSSIM, (b) MSE, (c) L1 Distance, and (d) KL-Divergence in relation to network accuracy. DSSIM exhibits consistent trends with accuracy, indicating a stronger rank correlation compared to the other metrics. The results highlight the significance of choosing appropriate attention similarity metrics.

transfer the attention outputs to the student and could be any distance metric. To choose a metric relevant to quantization accuracy, we randomly quantize a portion of attention heads in each MSA layer of the pretrained ViT-Base network and measure the attention head distance and network accuracy. We sample 500 settings from the configuration space and report Spearman and Kendall rank correlation coefficients. The comparison is shown in Fig. 5. The results show that DSSIM has the highest correlation with quantized accuracy.

According to the experimental results from Fig. 5, we choose DSSIM as  $g_{dist}$ . Therefore, the training objective  $\mathcal{L}_T$  of the quantized network is as follows:

$$\mathcal{L}_T = \mathcal{L}_{KL}(f_T(\hat{X})||f_S(\hat{X})) + \gamma\mathcal{L}_{HAD}, \quad (13)$$

where  $\hat{X}$  is synthetic samples,  $\gamma$  is a hyperparameter for  $\mathcal{L}_{HAD}$ .

## 6 Performance Evaluation

### 6.1 Experimental Settings

We evaluate MimiQ using three popular ViT architectures: ViT [14], DeiT [43], and Swin Transformer [32]. We report the quantization accuracy of tiny, small, and base versions of each architecture. MimiQ is compared with baseline methods on image classification, object detection, and semantic segmentation tasks. We employed the Timm library [1] for network implementation and its pretrained weights to benchmark on ImageNet [22] classification tasks. We conducted further comparisons on COCO [29] and ADE20K [52] datasets. For COCO dataset, we use Mask R-CNN [18] decoder with Swin Transformer backbone from mmdetection [6] library. For ADE20K dataset, we choose the UPerNet decoder with DeiT and Swin Transformer backbones from mmsegmentation [11] library. Pre-trained weights and network implementations were adopted from these libraries.

We used the Adam optimizer for the synthetic image generation with  $lr=0.1$  and  $b_1=0.9$ ,  $b_2=0.999$ . We used a batch size of 32, where each batch of synthetic samples was updated for 2K steps with an  $\alpha=1.0$  and  $\beta=2.5e-5$  following [47].

**Table 1:** Comparison on ImageNet image classification dataset.

Bits	Methods	Target Arch.	Networks								
			ViT-T	ViT-S	ViT-B	DeiT-T	DeiT-S	DeiT-B	Swin-T	Swin-S	Swin-B
W4/A4	Real-Data FT	-	58.17	67.21	67.81	57.98	62.15	64.96	73.08	76.34	73.06
	GDFQ	CNN	2.95	4.62	11.73	25.96	22.12	30.04	42.08	41.93	36.04
	Qimera	CNN	0.57	7.02	5.61	15.18	11.37	32.49	47.98	39.64	29.27
	AdaDFQ	CNN	2.00	1.78	6.21	19.57	14.44	19.22	38.88	39.40	32.26
	PSAQ-ViT	ViT	0.67	0.15	0.94	19.61	5.90	8.74	22.71	9.26	23.69
	PSAQ-ViT V2	ViT	1.54	4.14	2.83	22.82	32.57	45.81	50.42	39.10	39.26
	MimiQ (Ours)	ViT	<b>42.99</b>	<b>55.69</b>	<b>62.91</b>	<b>52.03</b>	<b>62.72</b>	<b>74.10</b>	<b>69.33</b>	<b>70.46</b>	<b>73.49</b>
	Acc. Gain		+40.04	+48.68	+51.18	+26.07	+30.15	+28.28	+18.91	+28.53	+34.23
	Real-Data FT	-	68.49	73.90	80.52	66.10	73.95	78.39	78.71	81.74	83.08
	GDFQ	CNN	24.40	53.96	33.56	44.76	57.00	71.03	61.30	78.04	70.55
Qimera	CNN	26.70	16.13	9.43	33.13	33.65	47.01	62.13	46.81	43.57	
AdaDFQ	CNN	27.10	59.36	43.02	53.85	59.55	71.12	64.61	79.82	75.59	
PSAQ-ViT	ViT	17.66	23.37	16.80	53.36	47.35	57.23	58.63	76.33	57.80	
PSAQ-ViT V2	ViT	40.21	63.59	74.29	55.18	65.30	73.16	69.77	80.55	79.80	
MimiQ (Ours)	ViT	<b>62.40</b>	<b>70.02</b>	<b>78.09</b>	<b>63.40</b>	<b>72.59</b>	<b>78.20</b>	<b>76.39</b>	<b>80.75</b>	<b>82.05</b>	
Acc. Gain		+22.19	+6.43	+3.80	+8.22	+7.28	+5.04	+6.63	+0.20	+2.25	
W4/A5	Real-Data FT	-	71.52	79.84	84.52	70.37	78.93	81.47	80.47	82.46	84.29
	GDFQ	CNN	62.65	76.06	81.68	65.82	76.49	80.03	78.90	81.47	83.63
	Qimera	CNN	61.80	60.08	63.22	61.90	70.10	72.38	73.93	72.22	76.35
	AdaDFQ	CNN	64.67	76.27	82.43	67.71	76.92	80.49	79.70	82.07	83.78
	PSAQ-ViT	ViT	59.59	62.98	67.74	66.16	76.56	80.05	79.06	81.89	79.51
	PSAQ-ViT V2	ViT	66.78	78.24	84.02	68.23	78.27	81.15	79.98	82.04	<b>83.90</b>
	MimiQ (Ours)	ViT	<b>68.15</b>	<b>78.77</b>	<b>84.20</b>	<b>69.86</b>	<b>78.48</b>	<b>81.34</b>	<b>80.06</b>	<b>82.08</b>	83.79
	Acc. Gain		+1.37	+0.53	+0.18	+1.63	+0.21	+0.20	+0.08	+0.01	-0.11
	Real-Data FT	-	74.83	81.30	85.13	71.99	79.70	81.77	80.96	83.08	84.79
	GDFQ	CNN	72.90	80.97	84.81	71.83	79.59	81.62	80.83	82.99	84.42
Qimera	CNN	72.88	81.04	84.98	71.76	79.46	81.58	80.41	82.95	84.37	
AdaDFQ	CNN	73.84	81.11	84.88	71.72	79.34	81.73	80.89	82.99	84.70	
PSAQ-ViT	ViT	72.73	81.17	84.89	<b>71.99</b>	<b>79.71</b>	81.79	<b>81.26</b>	<b>83.29</b>	<b>85.13</b>	
PSAQ-ViT V2	ViT	73.43	81.25	85.11	71.90	79.70	<b>81.86</b>	80.88	83.00	84.71	
MimiQ (Ours)	ViT	<b>74.60</b>	<b>81.30</b>	<b>85.17</b>	71.94	79.68	81.84	80.96	83.05	84.73	
Acc. Gain		+0.76	+0.05	+0.07	-0.05	-0.03	-0.02	-0.30	-0.24	-0.40	
W8/A8	Real-Data FT	-	74.83	81.30	85.13	71.99	79.70	81.77	80.96	83.08	84.79
	GDFQ	CNN	72.90	80.97	84.81	71.83	79.59	81.62	80.83	82.99	84.42
	Qimera	CNN	72.88	81.04	84.98	71.76	79.46	81.58	80.41	82.95	84.37
	AdaDFQ	CNN	73.84	81.11	84.88	71.72	79.34	81.73	80.89	82.99	84.70
	PSAQ-ViT	ViT	72.73	81.17	84.89	<b>71.99</b>	<b>79.71</b>	81.79	<b>81.26</b>	<b>83.29</b>	<b>85.13</b>
	PSAQ-ViT V2	ViT	73.43	81.25	85.11	71.90	79.70	<b>81.86</b>	80.88	83.00	84.71
	MimiQ (Ours)	ViT	<b>74.60</b>	<b>81.30</b>	<b>85.17</b>	71.94	79.68	81.84	80.96	83.05	84.73
	Acc. Gain		+0.76	+0.05	+0.07	-0.05	-0.03	-0.02	-0.30	-0.24	-0.40

Each synthetic dataset for fine-tuning comprises 10K samples. For fine-tuning the quantized networks, we use SGD optimizer with a Nesterov momentum of 0.9 with lr=1e-3, batch size of 16, and  $\gamma=\{1.0, 10.0, 100.0\}$ . The network is trained for 200 epochs and decay lr at epochs 50 and 100 by 0.1. We used min-max and LSQ [15] quantization methods and reported the best performance. We adapted data augmentations from SimCLR [7] for synthetic data generation and quantized network fine-tuning, such as ColorJitter, Gaussian Blur, etc.

## 6.2 Comparison on Image Classification Task

Tab. 1 shows the comparison of MimiQ against baseline DFQ methods. For comparison, we first provide “Real-Data FT” accuracies, which are from QAT with the original training dataset. Then, for the DFQ devised for CNN, we utilize all components that are applicable to ViT architecture. Lastly, for the DFQ methods for ViT, we utilize the official code from the authors.

**Table 2:** Comparison on semantic segmentation and object detection tasks.

Bits	Methods	COCO Dataset				ADE20K dataset			
		Swin-T		Swin-S		Backbones (mIoU)			
		AP <sub>box</sub>	AP <sub>mask</sub>	AP <sub>box</sub>	AP <sub>mask</sub>	DeiT-S	Swin-T	Swin-S	Swin-B
W4/A4	Real-Data FT	31.17	30.75	37.89	36.44	27.47	37.76	44.36	43.28
	PSAQ-ViT	0.06	0.06	0.05	0.06	0.15	1.65	3.30	0.89
	PSAQ-ViT V2	4.52	5.03	12.12	12.20	2.60	3.83	12.13	6.33
	MimiQ (Ours)	<b>26.41</b>	<b>26.63</b>	<b>34.97</b>	<b>33.53</b>	<b>17.20</b>	<b>29.92</b>	<b>38.29</b>	<b>36.40</b>
	Perf. Gain	+21.89	+21.60	+22.85	+21.33	+14.60	+26.09	+26.16	+30.07
W5/A5	Real-Data FT	42.98	39.66	46.61	42.18	33.10	40.13	47.14	47.43
	PSAQ-ViT	0.41	0.46	0.64	0.63	0.80	20.26	33.10	39.36
	PSAQ-ViT V2	32.69	31.21	45.20	40.99	5.35	26.35	37.58	42.01
	MimiQ (Ours)	<b>41.63</b>	<b>38.53</b>	<b>46.13</b>	<b>41.89</b>	<b>28.84</b>	<b>38.88</b>	<b>45.68</b>	<b>45.66</b>
	Perf. Gain	+8.94	+7.32	+0.93	+0.90	+23.49	+12.53	+8.10	+3.65
W4/A8	Real-Data FT	39.55	38.00	43.34	41.09	40.96	42.77	47.56	47.63
	PSAQ-ViT	33.45	32.97	37.57	36.35	35.73	41.25	46.42	46.70
	PSAQ-ViT V2	38.71	<b>37.59</b>	42.69	40.70	16.92	42.29	46.22	46.65
	MimiQ (Ours)	<b>38.77</b>	37.58	<b>42.77</b>	<b>40.87</b>	<b>41.18</b>	<b>43.24</b>	<b>46.91</b>	<b>47.49</b>
	Perf. Gain	+0.06	-0.01	+0.08	+0.17	+5.45	+0.95	+0.49	+0.79
W8/A8	Real-Data FT	46.01	41.63	48.29	43.13	41.96	43.62	46.16	45.39
	PSAQ-ViT	39.54	36.31	44.20	39.92	38.99	44.36	<b>47.68</b>	47.83
	PSAQ-ViT V2	45.84	41.51	48.17	43.22	19.51	44.26	47.56	47.68
	MimiQ (Ours)	<b>46.03</b>	<b>41.58</b>	<b>48.31</b>	<b>43.25</b>	<b>41.76</b>	<b>44.39</b>	47.62	<b>47.87</b>
	Perf. Gain	+0.19	+0.07	+0.14	+0.03	+2.77	+0.03	-0.06	+0.04

Overall, MimiQ shows significant accuracy gain across different quantization settings and network architectures, achieving a maximum gain of 51.18%p. In low-bit quantization settings, MimiQ shows significant improvement compared to the baselines. Moreover, there are some cases (DeiT-S/B, Swin-B) that MimiQ even outperforms Real-Data FT, due to the proposed structural attention head distillation. The results from higher bitwidth further support the effectiveness of our method. In the W5/A5 setting, MimiQ consistently outperforms the baselines in a notable margin up to 22.19%p. The results from the W4/A8 and W8/A8 settings show that MimiQ achieves similar performance compared to the Real-Data FT without access to any real samples.

In Tab. 1, the quantization accuracies of DeiT are significantly higher than that of similar-size ViTs. This may be due to the stronger inductive bias of DeiT, which makes it more robust against perturbations, thus helping the network preserve its capability under quantization noise. Swin Transformers also utilizes architectural inductive bias of locality and thus show greater performance.

### 6.3 Object Detection and Semantic Segmentation

We conduct further evaluations on object detection and semantic segmentation with various combinations of Transformer backbone and decoder architecture.

**Table 3:** Sensitivity analysis of hyperparameters.

$\alpha$	ViT-T	DeiT-T	ViT-B	DeiT-B	$\beta$	ViT-T	DeiT-T	ViT-B	DeiT-B	$\gamma$	ViT-T	DeiT-T	ViT-B	DeiT-B
0.01	41.41	41.22	37.09	54.07	2.5E-07	41.17	50.90	48.61	63.77	0.1	40.05	50.65	51.36	62.12
0.1	42.54	49.58	49.87	60.02	2.5E-06	41.19	50.85	48.61	63.13	1	42.67	52.03	53.96	63.11
1	42.67	52.03	53.96	63.11	2.5E-05	42.67	52.03	53.96	63.11	10	42.99	51.01	62.34	70.23
10	41.04	50.96	55.32	63.52	2.5E-04	41.56	48.36	51.27	63.13	100	36.48	44.34	62.91	74.10

First, we compare MimiQ with the baseline method on COCO dataset using Mask R-CNN decoder and Transformer backbones. We also evaluate on ADE20K datasets with Transformer backbones followed by a UPerNet decoder.

The experimental results on the COCO dataset are shown on the left-hand side of Tab. 2. The results show that MimiQ restores the quantization error of the Transformer backbone and CNN decoder by robustly outperforming the baseline in most settings. Similar to image classification evaluation, the performance gains in low-bit settings are highly noticeable, where achieving up to 22.85%p gain, while baseline methods make the network almost collapse.

Results on the ADE20K dataset (the right side of Tab. 2) further support that MimiQ performs well when applied to the Transformer backbone and CNN decoder combinations, showing great improvements on low-bit settings. The performance gains of the DeiT-S backbone are higher than those of other backbones, as the DeiT suffers from notably high performance drop compared to the Swin Transformer backbones. This is because DeiT architectures utilize weak inductive bias, while Swin Transformer architectures adapt the strong inductive bias of spatial locality. Therefore, DeiT backbones are vulnerable to quantization noise, as they need to preserve more information in their parameters.

#### 6.4 Sensitivity and Ablation Study

We conduct an ablation study of the individual effect of loss functions, shown in Tab. 4. In the first three rows, we show an ablation study regarding each component of  $\mathcal{L}_G$  ( $\mathcal{L}_{IHC}$ ,  $\mathcal{L}_{CL}$ , and  $\mathcal{L}_{TV}$ ) (Sec. 5.1). The first row shows the performance of the base synthesis method, which does not include the proposed loss

functions. We see accuracy drop when  $\mathcal{L}_{CL}$  is excluded, due to lack of crucial class information from pretrained classifier. As  $\mathcal{L}_{TV}$  only regularize steep changes across nearby pixels, it is the least significant generation loss affecting quantization accuracy. However, the overall trend shows that all generation losses cooperate to bring performance gain, showing the best accuracy when all losses are applied. On top of that, the proposed distillation  $\mathcal{L}_{HAD}$  (Sec. 5.2) further boosts the quantization accuracy, providing up to 23.24%p additional gain. Notably, the attention distillation method is particularly effective on larger models

**Table 4:** Ablation study of the loss functions on W4/A4 quantization setting.

$\mathcal{L}_G$			$\mathcal{L}_T$	Network			
$\mathcal{L}_{IHC}$	$\mathcal{L}_{CL}$	$\mathcal{L}_{TV}$	$\mathcal{L}_{HAD}$	ViT-T	DeiT-T	ViT-B	DeiT-B
✗	✓	✓	✗	13.28	37.70	7.72	34.84
✓	✗	✓	✗	12.31	16.29	0.59	6.78
✓	✓	✗	✗	38.38	50.21	37.80	56.88
✓	✓	✓	✗	39.61	50.16	39.67	62.11
✓	✓	✓	✓	42.99	52.03	62.91	74.10

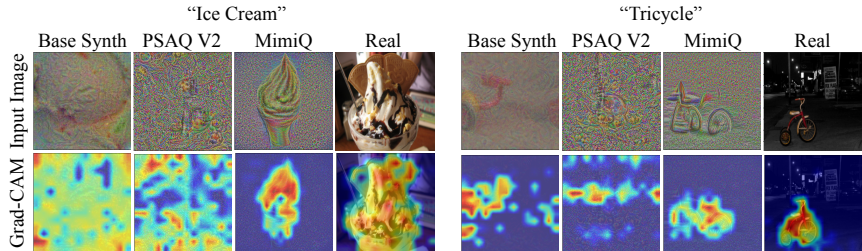


**Fig. 6:** Grad-CAM comparison of DFQ methods. We used gradient activation from the last layer of ViT-Base architecture.

(ViT/DeiT-B). We believe this is because the base models have more attention heads than tiny variants (Base:12, Tiny:3). Thus, head-wise distillation can provide more guidance from the full-precision counterpart.

In addition to the ablation study, we provide a sensitivity study on our hyperparameters in Tab. 3. We vary one hyperparameter while keeping others fixed at default. In line with the ablation study, each hyperparameter adds to final accuracy, with all results surpassing the baselines.

### 6.5 Inter-head Attention Similarity Metrics

We find that DSSIM has the highest correlation with quantized accuracy in Sec. 5.2. Here, we compare the quantization results from various choices of attention coherency metric  $g_{dist}$  in Tab. 5. The results show that attention head distillation improves performance regardless of the coherency metric. The trend is prominent in ViT-Base network, where +DSSIM achieves 14.29%p accuracy gain and (+MSE, +L1-Dist. +KL-Div.) get (5.23%p, 4.89%p, 1.29%p) improvements, which agree with the rank correlation coefficients order in Fig. 5. This indicates the clear advantage of DSSIM over other choices, which are mainly used for capturing distributional similarity or general magnitude difference.

**Table 5:** Performance comparison on coherency metric  $g_{dist}$ .

$g_{dist}$	Network			
	ViT-T	ViT-B	DeiT-T	DeiT-B
Baseline	39.61	39.67	50.16	62.11
+MSE	40.91	44.90	50.88	63.83
+L1-Dist.	40.57	44.56	50.60	63.97
+KL-Div.	39.63	40.96	50.33	62.59
+DSSIM	<b>42.99</b>	<b>62.91</b>	<b>52.03</b>	<b>74.10</b>

## 7 Discussion

### 7.1 Grad-CAM Analysis

As part of our analysis of how the MimiQ-generated images are viewed from the network’s perspective, we utilize Grad-CAM [41] to visualize the attention map from the last layer. From Fig. 6 which compares Grad-CAM of MimiQ against other data-free methods, it can be observed that MimiQ-generated images have most of its object information clear and well-clustered, similar to the real images. On the other hand, images from other methods have much of its object information scattered, which could harm the accuracy.

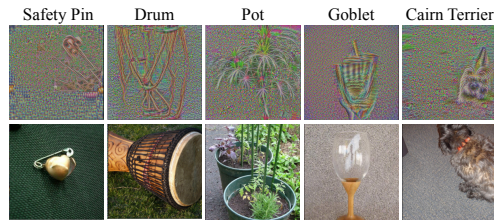


**Fig. 7:** To address potential societal concerns, similar pairs of images were found based on LPIPS value from ImageNet and synthetic images. There is no indication of privacy leaks.

**Table 6:** Experiments on two tasks to check if model inversion attack can be caused using ResNet-18. Results indicate that the attack fails.

Measure	Train	Test
Synthetic/Real Distinguishability	99.97	99.99
Synthetic→Real Transferability	49.69	0.16

## 7.2 Societal Concern

MimiQ may be considered as related to input reconstruction attacks [37, 44] which generate samples resembling the original dataset. To examine its potential risk, we used LPIPS to compare synthetic samples with the training dataset, as shown in Fig. 7. The upper images are synthetic samples from MimiQ, where the corresponding image below is a real sample with the lowest LPIPS value, which indicates that they form the most similar pair among the whole dataset. By observation, they capture general features of the class but do not replicate specific training images, demonstrating that MimiQ is far from having a serious threat of privacy leaks.

Following [38], we conducted two additional experiments using ResNet-18, depicted in Tab. 6. First, we trained the network to distinguish between real and synthetic samples. The average train and test accuracies are 99.97% and 99.99%, respectively, which means each are distinguishable from a perspective of the neural networks. This shows that MimiQ is hard to be considered as susceptible to identity attacks. We also evaluated a synthetic-trained network from scratch on a real dataset (ImageNet), which showed average train and test accuracies are 49.69% of 0.16%, respectively. This indicates such networks fail to learn significant information related to real datasets, reducing the risk of model inversion attacks.

## 8 Conclusion

In this paper, we propose MimiQ, a data-free quantization method for vision transformers inspired by attention similarity. MimiQ utilizes inter-head attention similarity to better leverage the knowledge instilled in the attention architecture, synthesizing training data that better aligns inter-head attention responses. In addition, MimiQ utilizes fine-grained head-wise attention map distillation from full-precision teacher to quantized counterpart. As a result, MimiQ brings significant performance gain, setting a new state-of-the-art DFQ method for Vision Transformer architectures.

## References

1. PyTorch Image Models, <https://timm.fast.ai/>
2. Banner, R., Nahshan, Y., Soudry, D.: Post training 4-bit quantization of convolutional networks for rapid-deployment. In: *Advances in Neural Information Processing Systems* (2019)
3. Brown, T., Mann, B., Ryder, N., Subbiah, M., Kaplan, J.D., Dhariwal, P., Neelakantan, A., Shyam, P., Sastry, G., Askell, A., et al.: Language models are few-shot learners. In: *Advances in Neural Information Processing Systems* (2020)
4. Cai, Y., Yao, Z., Dong, Z., Gholami, A., Mahoney, M.W., Keutzer, K.: ZeroQ: A novel zero shot quantization framework. In: *Proceedings of the IEEE/CVF Conference on Computer Vision and Pattern Recognition* (2020). <https://doi.org/10.1109/cvpr42600.2020.01318>
5. Cai, Z., He, X., Sun, J., Vasconcelos, N.: Deep learning with low precision by half-wave gaussian quantization. In: *Proceedings of the IEEE/CVF Conference on Computer Vision and Pattern Recognition* (2017). <https://doi.org/10.1109/cvpr.2017.574>
6. Chen, K., Wang, J., Pang, J., Cao, Y., Xiong, Y., Li, X., Sun, S., Feng, W., Liu, Z., Xu, J., Zhang, Z., Cheng, D., Zhu, C., Cheng, T., Zhao, Q., Li, B., Lu, X., Zhu, R., Wu, Y., Dai, J., Wang, J., Shi, J., Ouyang, W., Loy, C.C., Lin, D.: MMDetection: Open mmlab detection toolbox and benchmark. arXiv preprint arXiv:1906.07155 (2019). <https://doi.org/10.48550/arXiv.1906.07155>
7. Chen, T., Kornblith, S., Norouzi, M., Hinton, G.: A simple framework for contrastive learning of visual representations. In: *International Conference on Machine Learning* (2020)
8. Choi, K., Hong, D., Park, N., Kim, Y., Lee, J.: Qimera: Data-free quantization with synthetic boundary supporting samples. In: *Advances in Neural Information Processing Systems* (2021)
9. Choi, K., Lee, H.Y., Hong, D., Yu, J., Park, N., Kim, Y., Lee, J.: It’s all in the teacher: Zero-shot quantization brought closer to the teacher. In: *Proceedings of the IEEE/CVF Conference on Computer Vision and Pattern Recognition* (2022). <https://doi.org/10.1109/cvpr52688.2022.00813>
10. Choukroun, Y., Kravchik, E., Yang, F., Kisilev, P.: Low-bit quantization of neural networks for efficient inference. In: *IEEE/CVF International Conference on Computer Vision Workshop* (2019). <https://doi.org/10.1109/iccvw.2019.00363>
11. Contributors, M.: MMSegmentation: Openmmlab semantic segmentation toolbox and benchmark. <https://github.com/open-mmlab/mms Segmentation> (2020)
12. Courbariaux, M., Bengio, Y., David, J.P.: BinaryConnect: Training deep neural networks with binary weights during propagations. In: *Advances in Neural Information Processing Systems* (2015)
13. Devlin, J., Chang, M.W., Lee, K., Toutanova, K.: Bert: Pre-training of deep bidirectional transformers for language understanding. In: *North American Chapter of the Association for Computational Linguistics* (2019). <https://doi.org/10.18653/v1/N19-1423>
14. Dosovitskiy, A., Beyer, L., Kolesnikov, A., Weissenborn, D., Zhai, X., Unterthiner, T., Dehghani, M., Minderer, M., Heigold, G., Gelly, S., et al.: An image is worth 16x16 words: Transformers for image recognition at scale. In: *International Conference on Learning Representations* (2021)
15. Esser, S.K., McKinstry, J.L., Bablani, D., Appuswamy, R., Modha, D.S.: Learned step size quantization. In: *International Conference for Learning Representations* (2020)

16. Han, S., Mao, H., Dally, W.J.: Deep compression: Compressing deep neural networks with pruning, trained quantization and huffman coding. arXiv preprint arXiv:1510.00149 (2015). <https://doi.org/10.48550/arXiv.1510.00149>
17. Hathaliya, J.J., Tanwar, S.: An exhaustive survey on security and privacy issues in healthcare 4.0. *Computer Communications* (2020)
18. He, K., Gkioxari, G., Dollár, P., Girshick, R.: Mask r-cnn. In: Proceedings of the IEEE International Conference on Computer Vision. <https://doi.org/10.1109/iccv.2017.322>
19. Hubara, I., Courbariaux, M., Soudry, D., El-Yaniv, R., Bengio, Y.: Quantized neural networks: Training neural networks with low precision weights and activations. *The Journal of Machine Learning Research* (2017)
20. Jacob, B., Kligys, S., Chen, B., Zhu, M., Tang, M., Howard, A., Adam, H., Kalenichenko, D.: Quantization and training of neural networks for efficient integer-arithmetic-only inference. In: Proceedings of the IEEE/CVF Conference on Computer Vision and Pattern Recognition (2018). <https://doi.org/10.1109/cvpr.2018.00286>
21. Kong, Z., Dong, P., Ma, X., Meng, X., Niu, W., Sun, M., Shen, X., Yuan, G., Ren, B., Tang, H., et al.: Spvit: Enabling faster vision transformers via latency-aware soft token pruning. In: Computer Vision—ECCV 2022: 17th European Conference, Tel Aviv, Israel, October 23–27, 2022, Proceedings, Part XI (2022). [https://doi.org/10.1007/978-3-031-20083-0\\_37](https://doi.org/10.1007/978-3-031-20083-0_37)
22. Krizhevsky, A., Sutskever, I., Hinton, G.E.: Imagenet classification with deep convolutional neural networks. In: Advances in Neural Information Processing Systems (2012)
23. Li, Y., Xu, S., Zhang, B., Cao, X., Gao, P., Guo, G.: Q-vit: Accurate and fully quantized low-bit vision transformer. In: Advances in Neural Information Processing Systems (2022)
24. Li, Z., Chen, M., Xiao, J., Gu, Q.: Psaq-vit v2: Toward accurate and general data-free quantization for vision transformers. *IEEE Transactions on Neural Networks and Learning Systems* (2023). <https://doi.org/10.1109/tnnls.2023.3301007>
25. Li, Z., Gu, Q.: I-vit: integer-only quantization for efficient vision transformer inference. In: Proceedings of the IEEE/CVF International Conference on Computer Vision (2023). <https://doi.org/10.1109/ICCV51070.2023.01565>
26. Li, Z., Ma, L., Chen, M., Xiao, J., Gu, Q.: Patch similarity aware data-free quantization for vision transformers. In: Proceedings of the European Conference on Computer Vision (2022). [https://doi.org/10.1007/978-3-031-20083-0\\_10](https://doi.org/10.1007/978-3-031-20083-0_10)
27. Li, Z., Xiao, J., Yang, L., Gu, Q.: Repq-vit: Scale reparameterization for post-training quantization of vision transformers. In: Proceedings of the IEEE/CVF International Conference on Computer Vision (2023). <https://doi.org/10.1109/ICCV51070.2023.01580>
28. Lin, D., Talathi, S., Annapureddy, S.: Fixed point quantization of deep convolutional networks. In: International Conference on Machine Learning (2016)
29. Lin, T.Y., Maire, M., Belongie, S., Hays, J., Perona, P., Ramanan, D., Dollár, P., Zitnick, C.L.: Microsoft coco: Common objects in context. In: Proceedings of the European Conference on Computer Vision (2014). [https://doi.org/10.1007/978-3-319-10602-1\\_48](https://doi.org/10.1007/978-3-319-10602-1_48)
30. Lin, Y., Zhang, T., Sun, P., Li, Z., Zhou, S.: Fq-vit: Post-training quantization for fully quantized vision transformer. In: Proceedings of the Thirty-First International Joint Conference on Artificial Intelligence, IJCAI-22 (2022). <https://doi.org/10.24963/ijcai.2022/164>



31. Liu, B., Ding, M., Shaham, S., Rahayu, W., Farokhi, F., Lin, Z.: When machine learning meets privacy: A survey and outlook. *ACM Computing Surveys* (2021)
32. Liu, Z., Lin, Y., Cao, Y., Hu, H., Wei, Y., Zhang, Z., Lin, S., Guo, B.: Swin transformer: Hierarchical vision transformer using shifted windows. In: *Proceedings of the IEEE/CVF Conference on Computer Vision and Pattern Recognition* (2021). <https://doi.org/10.1109/iccv48922.2021.00986>
33. Liu, Z., Wang, Y., Han, K., Zhang, W., Ma, S., Gao, W.: Post-training quantization for vision transformer. *Advances in Neural Information Processing Systems* (2021)
34. Nagel, M., Amjad, R.A., Van Baalen, M., Louizos, C., Blankevoort, T.: Up or down? adaptive rounding for post-training quantization. In: *International Conference on Machine Learning* (2020)
35. Nagel, M., Baalen, M.v., Blankevoort, T., Welling, M.: Data-free quantization through weight equalization and bias correction. In: *Proceedings of the IEEE/CVF International Conference on Computer Vision* (2019). <https://doi.org/10.1109/iccv.2019.00141>
36. Nagel, M., Fournarakis, M., Amjad, R.A., Bondarenko, Y., van Baalen, M., Blankevoort, T.: A white paper on neural network quantization. *arXiv preprint arXiv:2106.08295* (2021). <https://doi.org/10.48550/arXiv.2106.08295>
37. Oh, H., Lee, Y.: Exploring image reconstruction attack in deep learning computation offloading. In: *The 3rd International Workshop on Deep Learning for Mobile Systems and Applications* (2019). <https://doi.org/10.1145/3325413.3329791>
38. Prakash, et al, P.: Privacy preserving facial recognition against model inversion attacks. In: *IEEE GLOBECOM* (2020). <https://doi.org/10.1109/globecom42002.2020.9322508>
39. Qian, B., Wang, Y., Hong, R., Wang, M.: Adaptive data-free quantization. In: *Proceedings of the IEEE/CVF Conference on Computer Vision and Pattern Recognition*. pp. 7960–7968 (2023). <https://doi.org/10.1109/CVPR52729.2023.00769>
40. Rastegari, M., Ordonez, V., Redmon, J., Farhadi, A.: XNOR-Net: Imagenet classification using binary convolutional neural networks. In: *Proceedings of the European Conference on Computer Vision* (2016). [https://doi.org/10.1007/978-3-319-46493-0\\_32](https://doi.org/10.1007/978-3-319-46493-0_32)
41. Selvaraju, R.R., Cogswell, M., Das, A., Vedantam, R., Parikh, D., Batra, D.: Grad-cam: Visual explanations from deep networks via gradient-based localization. In: *Proceedings of the IEEE International Conference on Computer Vision* (Oct 2017). <https://doi.org/10.1109/iccv.2017.74>
42. Sung, W., Shin, S., Hwang, K.: Resiliency of deep neural networks under quantization. *arXiv preprint arXiv:1511.06488* (2015). <https://doi.org/10.48550/arXiv.1511.06488>
43. Touvron, H., Cord, M., Douze, M., Massa, F., Sablayrolles, A., Jégou, H.: Training data-efficient image transformers & distillation through attention. In: *International Conference on Machine Learning* (2021)
44. Vepakomma, P., Singh, A., Zhang, E., Gupta, O., Raskar, R.: Nopeek-infer: Preventing face reconstruction attacks in distributed inference after on-premise training. In: *IEEE International Conference on Automatic Face and Gesture Recognition* (2021). <https://doi.org/10.1109/fg52635.2021.9667085>
45. Wang, Z., Bovik, A., Sheikh, H., Simoncelli, E.: Image quality assessment: from error visibility to structural similarity. *IEEE Transactions on Image Processing* (2004). <https://doi.org/10.1109/TIP.2003.819861>
46. Xu, S., Li, H., Zhuang, B., Liu, J., Cao, J., Liang, C., Tan, M.: Generative low-bitwidth data free quantization. In: *European Conference on Computer Vision* (2020). [https://doi.org/10.1007/978-3-030-58610-2\\_1](https://doi.org/10.1007/978-3-030-58610-2_1)

47. Yin, H., Molchanov, P., Alvarez, J.M., Li, Z., Mallya, A., Hoiem, D., Jha, N.K., Kautz, J.: Dreaming to distill: Data-free knowledge transfer via deepinversion. In: Proceedings of the IEEE/CVF Conference on Computer Vision and Pattern Recognition (2020). <https://doi.org/10.1109/cvpr42600.2020.00874>
48. Yu, H., Wu, J.: A unified pruning framework for vision transformers. *Science China Information Sciences* (2023). <https://doi.org/10.1007/s11432-022-3646-6>
49. Yuan, Z., Xue, C., Chen, Y., Wu, Q., Sun, G.: Ptq4vit: Post-training quantization for vision transformers with twin uniform quantization. In: European Conference on Computer Vision. pp. 191–207 (2022). [https://doi.org/10.1007/978-3-031-19775-8\\_12](https://doi.org/10.1007/978-3-031-19775-8_12)
50. Zhang, X., Qin, H., Ding, Y., Gong, R., Yan, Q., Tao, R., Li, Y., Yu, F., Liu, X.: Diversifying sample generation for accurate data-free quantization. In: Proceedings of the IEEE/CVF Conference on Computer Vision and Pattern Recognition (2021). <https://doi.org/10.1109/cvpr46437.2021.01540>
51. Zhong, Y., Lin, M., Nan, G., Liu, J., Zhang, B., Tian, Y., Ji, R.: Intraq: Learning synthetic images with intra-class heterogeneity for zero-shot network quantization. In: Proceedings of the IEEE/CVF Conference on Computer Vision and Pattern Recognition (2022). <https://doi.org/10.1109/cvpr52688.2022.01202>
52. Zhou, B., Zhao, H., Puig, X., Xiao, T., Fidler, S., Barriuso, A., Torralba, A.: Semantic understanding of scenes through the ade20k dataset. *International Journal of Computer Vision* (2019). <https://doi.org/10.1007/s11263-018-1140-0>
53. Zhou, S., Wu, Y., Ni, Z., Zhou, X., Wen, H., Zou, Y.: Dorefa-net: Training low bitwidth convolutional neural networks with low bitwidth gradients. arXiv preprint arXiv:1606.06160 (2016). <https://doi.org/10.48550/arXiv.1606.06160>
54. Zhu, B., Hofstee, P., Peltenburg, J., Lee, J., Alars, Z.: Autorecon: Neural architecture search-based reconstruction for data-free compression. In: International Joint Conference on Artificial Intelligence (2021). <https://doi.org/10.24963/ijcai.2021/478>